The Contribution of Stem Cell Factor and Granulocyte Colony-Stimulating Factor in Reducing Neurodegeneration and Promoting Neural Network Reorganization after Traumatic Brain Injury

Junchi He
State University of New York Upstate Medical University https://orcid.org/0000-0002-4662-3639
Thomas Russell
State University of New York Upstate Medical University
Xuecheng Qiu
State University of New York Upstate Medical University
Fei Hao
State University of New York Upstate Medical University
Michele Kyle
State University of New York Upstate Medical University
Lawrence Chin
State University of New York Upstate Medical University
Li-Ru Zhao (zhaol@upstate.edu)
https://orcid.org/0000-0002-9723-8124

Research article

Keywords: Traumatic brain injury; Stem cell factor; Granulocyte colony–stimulating factor; Neurodegeneration; Neural network reorganization; Functional recovery

Posted Date: February 18th, 2020

DOI: https://doi.org/10.21203/rs.2.17381/v2

Abstract

Background Traumatic brain injury (TBI) is a major cause of death and disability in young adults worldwide. TBI-induced long-term cognitive deficits represent a growing clinical problem. Stem cell factor (SCF) and granulocyte colony-stimulating factor (G-CSF) are involved in neuroprotection and neuronal plasticity. However, the knowledge concerning reparative efficacy of SCF+G-CSF treatment in post-acute TBI recovery remains incomplete. This study aims to determine the efficacy of SCF+G-CSF on post-acute TBI recovery in young adult mice. The controlled cortical impact model of TBI was used for inducing a severe damage in the motor cortex of the right hemisphere in 8-week-old male C57BL mice. SCF+G-CSF treatment was initiated 3 weeks after induction of TBI. Results Severe TBI led to persistent motor functional deficits (Rota-Rod test) and impaired spatial learning and memory (Morris water maze test). SCF+G-CSF treatment significantly improved the severe TBI-impaired spatial learning and memory 6 weeks after treatment. TBI also caused significant increases of Fluoro-Jade C positive degenerating neurons in bilateral frontal cortex, striatum and hippocampus, and significant reductions in MAP2 + apical dendrites and overgrowth of SMI312 + axons in peri-TBI cavity frontal cortex and in the ipsilateral hippocampal CA1 at 24 weeks post-TBI. SCF+G-CSF treatment significantly reduced TBI-induced neurodegeneration in the contralateral frontal cortex and hippocampal CA1, increased MAP2 + apical dendrites in the peri-TBI cavity frontal cortex, and prevented TBI-induced axonal overgrowth in both the peri-TBI cavity frontal cortex and ipsilateral hippocampal CA1. Conclusions These findings reveal a novel pathology of axonal overgrowth after TBI and demonstrate a therapeutic potential of SCF+G-CSF in ameliorating TBI-induced long-term neuronal pathology, neural network malformation, and impairments in spatial learning and memory.

Background

As a growing clinical problem around the world, traumatic brain injury (TBI) remains the leading cause of death and disability in young adults [1]. The pathological period of post-TBI is divided into 3 phases: an acute phase, a subacute phase, and a chronic phase. The precise duration of the 3 clinical phases is different for individuals because many factors may affect the pathological time course such as their ages and TBI severity. Generally, the acute phase is the first 7 days after TBI, the subacute phase is between 7 days and 3 weeks after TBI, and the chronic phase begins 3 to 5 weeks after TBI [2-5]. To date, the majority of pre-clinical studies have focused on pharmaceutical interventions in neuroprotection in the acute phase of TBI, such as complement inhibition [6], immunomodulation [7], angiotensin II receptor blockage [8], and cerebral infusion of insulin-like growth factor-1 [9]. However, little work has been done in exploring pharmaceutical approaches in post-acute phases of TBI.

The process of the secondary brain injury is progressive, and secondary neuron loss happens in both the ipsilateral and contralateral hemispheres. A recent study has revealed a long-term and progressive neuropathology in bilateral hemispheres up to one year after a single severe TBI in mice [10]. Moreover, progressive neurodegeneration after TBI has been found in both the ipsilateral and contralateral hemispheres [11, 12]. Widespread neurodegeneration after TBI has been thought to be the results of

secondary brain injury and lead to cognitive impairments [13]. In addition to widespread neurodegeneration, reduced functional connectivity in both hemispheres has also been observed in TBI patients [14]. TBI-induced loss of dendrites and axons is also related with cognitive impairments [15, 16]. The pharmaceutical intervention for inhibiting widespread neurodegeneration and enhancing neural network reorganization may restrict TBI-induced progressive neuropathology and improve functional outcomes after TBI.

Stem cell factor (SCF) and granulocyte colony-stimulating factor (G-CSF) are the key hematopoietic growth factors to regulate bone marrow stem cell proliferation, differentiation and mobilization [17-20]. Accumulating evidence shows that SCF and G-CSF also play a role in neuroprotection and neuronal plasticity. Many studies have demonstrated that administration of SCF [21], G-CSF [21-26], or SCF+G-CSF [21, 27, 28] leads to reduction in infarction size and amelioration of neurological deficits in experimental stroke. In addition to neuroprotection, SCF has been shown to promote neurite outgrowth [29, 30], and lack of SCF impairs spatial and learning memory [31]. G-CSF deficient mice also show cognitive problems, impairments in long-term potentiation, and reductions in dendrites in the hippocampus [32]. SCF and G-CSF have been demonstrated to cross the blood-brain barrier in intact animals [33]. SCF and G-CSF combined treatment (SCF+G-CSF) has shown synergistic effects in enhancing neurite outgrowth [34] and neural network reorganization in chronic stroke [30]. We have also demonstrated that SCF+G-CSF treatment in the chronic phase of experimental stroke synergistically improves functional recovery [30]. SCF+G-CSF-improved functional recovery in the chronic phase of experimental stroke is dependent on the SCF+G-CSF-enhanced neural network remodeling [35, 36]. Our previous study has revealed that systemic administration of SCF+G-CSF at 2 weeks post-TBI improves functional outcomes and ameliorates TBI-induced neurodegeneration and dendrites loss [37]. However, it remains unexplored whether this pharmaceutical approach is effective at the late stage of TBI. The knowledge concerning reparative efficacy of SCF+G-CSF treatment in late subacute phase of TBI remains incomplete.

The aim of the present study is to determine the efficacy of SCF+G-CSF treatment at the late subacute stage of TBI in brain repair and functional recovery.

Methods

The animal experiments followed ethical guidelines of the Animal Research, Reporting In Vivo Experiments (ARRIVE). All procedures in this study were approved by the Institutional Animal Care and Use Committee and performed in accordance with the Guide for the Care and Use of Laboratory Animals by the National Institutes of Health.

Animals and Experimental Design

A total of 30 male C57BL/6J mice (8 weeks old) (The Jackson Laboratory Co., Bar Harbor, Maine, US) were used for this study. These mice were housed in a 12-h light/dark cycle with food and water available *ad libitum*.

Three weeks after induction of TBI, mice were randomly divided into two groups: a vehicle control group (n=11) and an SCF+G-CSF-treated group (n=12). Mice without TBI served as sham operative controls (n=7). SCF+G-CSF or an equal volume of vehicle solution were subcutaneously injected for 7 consecutive days starting on day 21 post-TBI. The dosage and treatment paradigm were selected according to our earlier studies in chronic stroke [35, 38].

Neurobehavioral tests were performed for determination of neurological deficits one week before treatment as well as 2 and 6 weeks after treatment (Figure 1A).

Controlled Cortical Impact Murine Model of TBI

Controlled cortical impact (CCI) model was used to induce severe TBI. Mice were anesthetized with Avertin (Sigma) (0.4g/kg, i.p.) and placed in a head holder, where the head of the mouse was immobilized with two ear bars and a tooth bar. A midline cranial incision was made, and the skull was exposed. A 4-mm-in-diameter circle with a central point of 2mm lateral to the bregma was drawn on the right side of the skull (somatosensorimotor cortex of the forelimb and hindlimb in mice). A craniotomy was performed following the circle with a dental drill. The skull was carefully removed without damaging the dura. The mouse was then subjected to TBI through the IH-0400 Impactor (Precision Systems and Instrumentation Co.) with a 3-mm-in-diameter round tip at 125 kdyne force level, and force curves recorded for abnormalities in impact using PSI-IH Impactor software. The skull flap was then placed over the craniotomy without adhesive due to concerns of increasing intracranial pressure. The wound was closed with 3-0 prolene sutures. Sham mice were operated in the same procedure except the cortex was not impacted.

Administration of Stem Cell Factor and Granulocyte-Colony Stimulating Factor

Recombinant mouse SCF (PeproTech) was diluted with saline, and recombinant human G-CSF (Amgen) was diluted with 5% dextrose. SCF (200μg/kg/day) and G-CSF (50μg/kg/day) were injected subcutaneously for 7 consecutive days at 24-hour intervals to the mice in TBI- SCF+G-CSF group. The location of the injection was on the backside of the neck. Due to the small volume and difficulty with maintaining the mice in appropriate position during injection, mice were anesthetized with isoflurane to ensure proper subcutaneous injection. An equal volume of vehicle solution (50% of saline with 50% of dextrose) was subcutaneously injected to the mice in the TBI-vehicle group.

Morris Water Maze Test

The Morris water maze testing was performed in a water tank with 4 quadrants and a hidden platform placed in quadrant IV. Mice were tested for a total of 8 trials, 2 in each quadrant every day. Each trial ended with either the maximum time limit of 60 seconds or when the mouse found the platform. The mice were placed in quadrant I at the beginning of each trial and followed a fixed order of I, II, III, IV, and I, II, III, IV. The testing was performed over the course of 5 days. Trials were performed early in the morning within a 1-hour time frame each day, with a 1-hour acclimation period to the testing room before testing

would begin. The latency to find the platform and the distance the animal traveled were recorded through ANY-Maze Video Tracking System (Stoelting Co.).

Rota-Rod Test

Mice were placed on Rota-Rod (Coulbourn Instrument) for testing motor function. Once all 5 mice were set, start button was pressed. The speed of the Rota-Rod was set as starting at 4 rpm and ending at 40 rpm with a maximum 5 min duration (by increasing 4 rpm every 30 sec). The test ended at 5 min or when the mouse fell. The testing was repeated 3 times with at least 15 minutes of rest between each trial. The latency to fall from Rota-Rod was recorded.

Brain Section Preparation

At 24 weeks after TBI (i.e. 20 weeks post-treatment), mice were anesthetized with overdose of Avertin (Sigma) (0.4 g/kg, i.p.) and transcardially perfused with phosphate buffered saline (PBS) (50 ml) followed by 4% formaldehyde (Sigma) (50 ml). The brains were excised and immediately immersed in 4% formaldehyde for 24 h for post-fixation and then cryoprotected in 30% sucrose in PBS for 2 days. The brains were then sectioned into 30-mm-thick sections with a microtome (American Optical Corp.).

Fluoro-Jade C Staining

Brain sections (2-4 sections/brain) at the level 1.10 mm anterior to bregma and 1.10 mm posterior to bregma (Figure 1B) were mounted on Superfrost Plus Slides (Fisher Scientific) and allowed to dry overnight at room temperature. The slides were immersed in 100% ethanol then 70% ethanol. Brain sections were then rinsed in distilled water and immersed in 0.06% potassium permanganate (Sigma). After being rinsed in distilled water, the slides were incubated with 0.001% Fluoro-Jade C (Millipore) for 30 min, dried at room temperature overnight in the dark, cleared by brief immersion in xylene, and mounted with DepeX mounting media (Elextron Microscopy Sciences). Images of the cortex at 500 μm away from the TBI cavity, the corresponding area in the contralateral cortex, and bilateral striatum and CA1 (Figure 1B) were captured with a 20x objective using a confocal fluorescence microscope (Zeiss LSM780, Germany). Fluoro-Jade C-positive staining was analyzed by Image J software.

Immunohistochemistry

Free-floating technique was used for immunohistochemistry. Briefly, brain sections (3-4 adjacent sections/brain) at the level 1.00 mm anterior to bregma and 1.10 mm posterior to bregma (Figure 1B) were chosen for immunohistochemistry. The sections were rinsed with PBS, incubated in solution of PBS-diluted 10% normal goat serum (NGS), 1% bovine serum albumin (BSA), and 0.3% Triton X-100 for 1 hour at room temperature to block non-specific binding. The sections were then incubated with the primary antibody polyclonal rabbit anti-microtubule associated protein 2 (MAP2, 1:600, Millipore), monoclonal mouse anti-SMI312 (1:500, Biolegend), monoclonal mouse anti-NeuN (1:500, Millipore), or polyclonal rabbit anti-amyloid precursor protein (APP) (CT695) (1:100, ThermoFisher) in PBS solution with 1% BSA

and 0.3% Triton X-100 overnight at 4^{o} C. In negative control brain sections, the primary antibodies were omitted. The next day the sections were washed with PBS and incubated with the secondary antibody DyLight 488-labeled goat anti-rabbit, DyLight 488-labeled goat anti-mouse, or Dylight 594-labeled goat anti-rabbit in PBS solution with 1% BSA and 0.3% Triton X-100. Sections were rinsed with PBS again and then mounted on Superfrost Plus Slides and coverslipped with Vectashield Antifade Mounting Medium (Vector Laboratories). Confocal images of MAP2 immunofluorescence staining in cortical layer 1and layer 2 (500μm away from the TBI cavity) as well as the stratum radiatum (RAD) and stratum lacunosum moleculare (LM) of hippocampus CA1 in both the ipsilateral hemisphere and corresponding contralateral sites (Figure 1B) were taken with a confocal fluorescence microscope (Zeiss LSM780, Germany). Confocal images of SMI312 immunofluorescence staining in cortical layer 1-5 (500 μm away from the TBI cavity) and in the hippocampal CA1 of both the ipsilateral hemisphere and corresponding contralateral site (Figure 1B) were taken with the confocal fluorescence microscope. Confocal images of NeuN immunofluorescence staining in the cortical layer 2 and layer 3 at 500 μm away from the TBI cavity, the corresponding area in the contralateral cortex, and bilateral CA1 (Figure 1B) were taken with the Zeiss confocal microscope. Confocal images of APP immunofluorescence staining at layer 2 and layer 3 cortex at 500 μm away from the TBI cavity, the corresponding area in the contralateral cortex, bilateral CA1, and bilateral corpus callosum were taken with the Zeiss confocal microscope. The Integrated optic densities of MAP2 positive dendrites, MAP2 positive area (%), SMI312 positive area (%), and the percentage of NeuN positive neurons in total of DAPI positive cells were analyzed by Image J software.

Tissue Loss Volume Determination

Serial coronal brain sections (30 μm thickness at 15 section intervals) were taken and processed for Hematoxylin and Eosin (H&E) staining. Briefly, brain sections were rehydrated, washed with tap water, subjected to hematoxylin stain for 1-2 minutes. The sections were washed with tap water again and dipped in ammonia water until blue. The sections were then washed with tap water and 95% alcohol until the slide cleared, subjected to eosin for 10 seconds, dehydrated, and mounted in xylene based medium. The measurement of the width and the depth of the cavity through cross sections were cumulated to calculate the volume of the cavity. Briefly, the area of tissue loss was calculated by subtracting the ipsilateral remaining hemisphere from the contralateral hemisphere in each section. The volume of tissue loss was calculated by multiplying the mean area of tissue loss by the number of sections and the thickness of each section. The volume of tissue loss was then divided by the volume of contralateral hemisphere to get the percentage of tissue loss.

Statistical Analysis

Statistical analysis was performed using Prism (GraphPad) software. Shapiro-Wilk’s normality test was used to assess normality. No data was significantly different than the Gaussian distribution. Student’s t-test was used to analyze pretreatment behavioral data and tissue loss volume between two experimental groups. A one-way ANOVA was utilized to analyze Fluoro-Jade C and immunohistochemical data among three experimental groups. A two-way repeated measures ANOVA was used to evaluate time and

treatment differences for the data collected from Morris water maze and Rota-Rod testing. Tukey's *post hoc* analysis was used to compare the differences between groups. Significance was set at $P < 0.05$.

Results

SCF+G-CSF treatment does not improve TBI-impaired cognitive and motor functions 2 weeks after treatment

To ensure that TBI mice presented equal pathological conditions in the treated and non-treated groups before the SCF+G-CSF treatment initiation, we examined cognitive and motor functional deficits one week before treatment by Morris water maze test and Rota-Rod test, respectively. The latency to find the platform was longer in all TBI mice than in sham control mice ($P < 0.01$) (Additional file figure 1A). TBI mice were then randomly divided into two groups: a TBI-vehicle control group and a TBI-SCF+G-CSF-treated group. The escape latency did not show any difference between the two experimental groups (Additional file figure 1B). A similar findings was found in a 3-day pretesting Rota-Rod (Additional file figure 1C, D). These findings demonstrate the equal pathological conditions in the TBI-vehicle control group and TBI-SCF+G-CSF treatment group before the treatment initiation.

To determine the efficacy of SCF+G-CSF on cognitive and motor functional recovery, we performed Morris water maze and Rota-Rod tests 2 weeks after the treatment, respectively. In Morris water maze test, the escape latency was longer on day 4 and day 5 in TBI-vehicle control mice when compared with sham-operated mice ($P < 0.05$). There was no significant difference in the escape latency between TBI-vehicle controls and TBI-SCF+G-CSF-treated mice (Figure 2A). In Rota-Rod test, the latency to fall was reduced in TBI-vehicle control mice as compared to sham mice from day 2 to day 5 ($P < 0.05$). There was no significant difference between the TBI-vehicle group and the TBI-SCF+G-CSF group (Figure 2B). These data indicate that SCF+G-CSF treatment does not improve spatial learning and memory and motor function at 2 weeks post-treatment.

SCF+G-CSF treatment improves TBI-impaired cognitive function but not motor function 6 weeks after treatment

Next, we examined the long-term effects of SCF+G-CSF treatment on cognitive and motor functional recovery after TBI. Morris water maze and Rota-Rod tests were carried out 6 weeks after treatment.

In the Morris water maze, we found that the escape latency to platform was increased in the TBI-vehicle mice on day 1 ($P < 0.05$), day 4 ($P < 0.05$) and day 5 ($P < 0.01$) as compared with sham controls (Figure 2C), indicating that TBI leads to a long-term impairment in spatial learning and memory. The SCF+G-CSF-treated TBI mice, however, showed a significant reduction in escape latency when compared to the TBI-vehicle control mice on day 5 ($P < 0.01$, Figure 2C).These data suggest that SCF+G-CSF treatment improves TBI-impaired long-term spatial learning and memory.

In Rota-Rod test, TBI-vehicle control mice showed a decrease in latency to fall in comparison with sham controls on days 1, 2, 3 and 5 ($P < 0.05$). The latency to fall in TBI-SCF+G-CSF-treated mice did not differ from TBI-vehicle controls (Figure 2D). These findings suggest that SCF+G-CSF-treatment is insufficient in improving motor function after severe TBI.

SCF+G-CSF treatment does not influence the tissue loss volume after TBI

To examine whether SCF+G-CSF treatment influences the total tissue loss after TBI, we assessed the total tissue loss volume using H&E staining 20 weeks after SCF+G-CSF treatment. Our data showed that there was no significant difference in the volume of brain tissue loss between TBI-vehicle controls and TBI-SCF+G-CSF-treated mice ($P > 0.05$) (Additional file figure 2).

SCF+G-CSF treatment prevents TBI-induced neurodegeneration in the contralateral cortex and hippocampal CA1

In a closed-head impact TBI model, chronic traumatic encephalopathy was detected at 5.5 months post-injury [39]. In a mouse model of mild TBI, neurodegeneration was limited to the cortex 2 months after TBI, but neurodegeneration was detected in both the cortex and hippocampus at 6 months post-TBI [40]. Therefore, we chose 20 weeks after treatment (i.e. 24weeks after TBI) as the time point to evaluate neurodegeneration in the cortex, hippocampus and striatum.

To investigate the effect of SCF+G-CSF on long-term neurodegeneration after TBI, we performed Fluoro-Jade C staining 20 weeks after treatment. Fluoro-Jade C positive cells were increased in TBI-vehicle mice as compared with sham controls in both the ipsilateral ($P < 0.05$) and contralateral cortex ($P < 0.01$), in both the ipsilateral ($P < 0.01$) and contralateral striatum ($P < 0.05$), and in both the ipsilateral ($P < 0.05$) and contralateral CA1 ($P < 0.01$) (Figure 3 A-I), suggesting that the severe TBI causes a long-term neurodegeneration in both the ipsilateral and contralateral hemispheres. SCF+G-CSF treatment significantly reduced the number of Fluoro-Jade C positive cells in the contralateral cortex ($P < 0.05$) and CA1 ($P < 0.05$) as compared with TBI-vehicle control mice (Figure 3A, C, D and H). Although significant differences between the treated and non-treated TBI mice in the ipsilateral hemisphere were not seen, the Fluoro-Jade C positive cells in the ipsilateral cortex next to the TBI cavity and striatum were found no significant differences between the SCF+G-CSF-treated TBI mice and sham controls (Figure 3 E and G). These findings indicate that SCF+G-CSF treatment ameliorates severe TBI-induced long-term neurodegeneration, particularly in the contralateral cortex and hippocampal CA1.

We also analyzed neuronal loss in bilateral cortex and hippocampal CA1 by quantifying the percentage of NeuN positive cells in total of DAPI positive cells (Additional file figure 3 A-F). Surprisingly, the percentage of NeuN positive cells in the contralateral cortex and hippocampal CA1 was no difference among the sham controls, TBI control mice, and TBI mice treated with SCF+G-CSF (Additional file figure 3A, B, D, and E). The discrepancies between total degenerating neurons (Fluoro-Jade C positive) and survival neurons (NeuN positive cells) observed in the contralateral cortex and hippocampal CA1 suggest that the neuron degeneration in the contralateral hemisphere may be still in progressive process at which stage it has not

reached the pathological levels to kill the neurons. By contrast to the findings in the contralateral hemisphere, NeuN positive cells in the ipsilateral cortex and hippocampal CA1 showed a similar pattern that was seen in the findings of Fluoro-Jade C positive cells in the same regions. The NeuN positive cells in the ipsilateral cortex next to the TBI cavity and the ipsilateral hippocampal CA1 were significantly reduced in the TBI-vehicle control mice as compared to the sham controls ($P < 0.05$, Additional file figure 3A, C, D, and F), whereas the NeuN positive cells were found no significant difference between TBI-vehicle controls and SCF+G-CSF-treated TBI mice, as well as between SCF+G-CSF-treated TBI mice and sham controls (Additional file figure 3 A, C, D, and F). These findings suggest that severe TBI may trigger a severe pathological cascade of neurodegeneration in the ipsilateral hemisphere resulting in neuron loss in the peri-TBI cavity cortex and ipsilateral hippocampal CA1.

SCF+G-CSF treatment increases apical dendritic density in the ipsilateral cortex after TBI

We then sought to determine the efficacy of SCF+G-CSF treatment in remodeling of dendritic branching after TBI. In the contralateral cortex, we did not found any differences in MAP2 positive dendrites (MAP2 positive dendritic optic density and MAP2 positive area) between sham controls, TBI-vehicle control mice, and SCF+G-CSF-treated TBI mice ($P > 0.05$) (Figure 4 A-E). In the ipsilateral cortex adjacent to the TBI cavity, however, TBI-vehicle mice showed significant reductions in MAP2 positive dendritic apical density in layer 1 ($P < 0.01$) and layer 2 ($P < 0.001$) as compared to sham-operated mice. This observation was further validated by analysis of MAP2 immunopositive area (TBI-vehicle controls vs. sham controls: $P < 0.01$ in both ipsilateral layer 1 and 2). These findings indicate that severe TBI leads to a long-term dendrites reduction in the ipsilateral cortex. SCF+G-CSF treatment, however, significantly increased MAP2 positive apical dendrites (MAP2 positive dendritic optic density and MAP2 positive area) in both layer 1 ($P < 0.05$) and layer 2 ($P < 0.05$) of the ipsilateral cortex next to the TBI cavity in comparison with TBI-vehicle controls (Figure 4F-J), suggesting that SCF+G-CSF treatment ameliorates TBI-reduced dendritic density in the peri-TBI cortex.

In the contralateral hippocampus, we did not observe any differences in MAP2 positive dendrites (MAP2 positive dendritic optic density and MAP2 positive area) among sham controls, TBI-vehicle control mice, and SCF+G-CSF-treated TBI mice in both the RAD CA1 and LM CA1 regions ($P > 0.05$) (Figure 5A-C, and F-H). However, in the ipsilateral hippocampus, the MAP2 positive dendritic optic density in TBI-vehicle control mice was significantly decreased in RAD CA1 ($P < 0.05$, Figure 5D) and LM CA1 ($P < 0.01$, Figure 5I) as compared to sham controls. These data were further confirmed by analysis of MAP2 positive area (TBI-vehicle controls vs. sham controls: $P<0.01$ in RAD CA1, Figure 5E; $P < 0.05$ in LM CA1, Figure 5J). These findings indicate a long-term decrease in dendritic density in the ipsilateral hippocampus by severe TBI. We did not see any increases of MAP2 positive dendritic optic density (Figure 5D and I) and MAP2 positive area(Figure 5E and J) in the ipsilateral RAD or LM CA1 after SCF+G-CSF treatment, suggesting that SCF+G-CSF does not modify the TBI-induced long-term reduction of dendrites in the ipsilateral hippocampus.

SCF+G-CSF treatment prevents TBI-induced overgrowth of axons in the ipsilateral cortex and hippocampus

To determine whether SCF+G-CSF treatment modifies axonal density after TBI, we analyzed SMI312 immunopositive axons in both the cortex and hippocampus 20 weeks after treatment (i.e. 24 weeks post-TBI).

In the contralateral cortex, the SMI312 positive axons in layer 1 were significantly increased in TBI-vehicle mice as compared to the sham controls ($P < 0.05$) (Figure 6A and B). TBI-vehicle mice also showed a trend toward increasing SMI312 positive axons in layer 2-3 ($P = 0.081$, Figure 6C) and layer 4-5 ($P = 0.066$, Figure 6D) in comparison with sham controls. SCF+G-CSF-treated TBI mice displayed a trend toward decreasing SMI312 positive axons in layer 1 ($P = 0.087$, Figure 6B) as compared to the TBI-vehicle control mice.

In the ipsilateral cortex next to the TBI cavity, TBI-vehicle mice showed significant increases in SMI312 positive axons in layer 1 ($P < 0.05$, Figure 6B), layer 2-3 ($P < 0.05$, Figure 6C), and layer 4-5 ($P < 0.01$, Figure 6D) when compared to sham controls, demonstrating a TBI-induced long-term overgrowth of axons in the ipsilateral cortex. SCF+G-CSF treatment, however, significantly reduced SMI312 positive axons in layer 2-3 ($P < 0.01$, Figure 6C), and layer 4-5 ($P < 0.05$, Figure 6D) as compared to TBI-vehicle control mice. A trend toward decreasing SMI312 positive axons in layer 1 ($P = 0.068$, Figure 6B) was also observed in SCF+G-CSF-treated TBI mice as compared to the TBI-Vehicle control mice. This observation suggests that the TBI-induced long-term overgrowth of axons in the peri-TBI cortex is inhibited by SCF+G-CSF treatment.

In the contralateral hippocampus, differences in SMI312 positive axons in the CA1 region were not seen among sham controls, TBI-vehicle control mice, and SCF+G-CSF-treated TBI mice (Figure 7A and B). In the ipsilateral hippocampus, however, TBI-vehicle mice showed a significant increase in SMI312 positive axons in CA1 ($P < 0.05$, Figure 7C) as compared to sham controls. SCF+G-CSF treatment significantly decreased SMI312 positive axons in the ipsilateral CA1 when compared to TBI-vehicle control mice ($P < 0.05$, Figure 7C). No difference was seen between TBI-SCF+G-CSF-treated mice and sham controls. These findings indicate that TBI-induced long-term overgrowth of axons in the ipsilateral hippocampus is prevented by SCF+G-CSF treatment.

To investigate axonal injury in the late subacute phase of TBI, we performed APP immunohistochemistry to identify axonal injury at 24 weeks post-TBI. Our data showed that there were no APP positive axons in the ipsilateral and contralateral corpus callosum, cortex, and CA1 (Additional file figure 4 A-C). As a control, we also performed APP immunohistochemistry in the brain sections collected from 7 days after TBI. We observed APP immunopositive staining in the ipsilateral corpus callosum and peri-TBI cortex 7 days after TBI. No APP positive staining was seen in the ipsilateral CA1, the contralateral corpus callosum, the contralateral cortex, and the contralateral CA1 at 7 days post-TBI (Additional file figure 4D). These data indicate that TBI does not induce APP expression in the injured axons in the late subacute

phase of TBI. Traumatic axonal injury may occur only at the early stage of TBI but not at the late stage of TBI.

Discussion

In the present study, we have demonstrated that the combination treatment of SCF and G-CSF at the late subacute stage of TBI (3 weeks post-TBI) ameliorates severe TBI-induced long-term impairments in spatial learning and memory, reduces neurodegeneration, and enhances neural network structural reorganization.

SCF+G-CSF treatment improves spatial learning and memory 6 weeks, but not 2 weeks, after treatment in a severe CCI-TBI model. This observation suggests that SCF+G-CSF requires a prolonged period (6 weeks) to repair the brain damaged by severe TBI. This finding is in line with the data of previous publications. SCF+G-CSF treatment post-acute TBI improves spatial learning and memory in water maze testing 6 weeks after treatment [41]. Using a cortical ischemia model of stroke, Kawada and coworkers have revealed that SCF+G-CSF treatment during 11-20 days after cortical ischemia leads to improvements of spatial learning and memory in water maze test at 4 weeks post-stroke [27]. The question as to why the SCF+G-CSF treatment improves recovery of spatial learning and memory in a delayed time remains to be addressed in future studies. In this study, we have also observed that SCF+G-CSF treatment fails to improve motor functional recovery in the severe CCI-TBI model. This may be due to the severe damage in the motor cortex by the CCI-TBI model. This finding is also consistent with our previous observation that persistent impairments in motor function by severe CCI-TBI are not improved by SCF+G-CSF treatment [41]. Although SCF+G-CSF treatment at 3 weeks post-TBI has no effect on improving motor function or on reducing lesion size in our severe CCI-TBI model, the findings of SCF+G-CSF-improved spatial learning and memory recovery suggest that the reparative processes may occur in the remaining brain regions remote from or next to the TBI-damaged motor cortex.

We have observed that the TBI-induced neurodegeneration in the contralateral cortex and hippocampal CA1 is prevented by SCF+G-CSF treatment. Accumulating evidence has demonstrated that a moderate or severe CCI-TBI causes widespread, progressive, and long-term neurodegeneration [42, 43]. Progressively increased neuron loss has been found at 5, 12, and 52 weeks post-CCI-TBI as compared to one week after injury [42]. In the present study, we have revealed that widespread degenerating neurons are increased in the cortex, striatum, and hippocampal CA1 in both hemispheres 24 weeks after severe CCI-TBI. It has been shown that the widespread neurodegeneration after TBI is tightly linked to cognitive impairments [13, 44]. The present study has demonstrated that SCF+G-CSF ameliorates long-term neurodegeneration in the contralateral frontal cortex and hippocampus remote from the injury site in the late subacute phase of TBI. This observation is consistent with our previous study showing that SCF+G-CSF intervention prevents TBI-induced neurodegeneration in the contralateral hemisphere in the subacute phase of TBI [37]. In the present study, neuron loss was observed only in the peri-TBI cavity cortex and the ipsilateral hippocampal CA1, but not in the contralateral cortex and CA1, indicating that neurons in the contralateral areas may be sub-lethally injured. These sub-lethally injured neurons undergo degeneration that could be

inhibited by SCF+G-CSF treatment. Whether increased dose or prolonged treatment would significantly reduce neurodegeneration in the ipsilateral hemisphere remains to be addressed. Although the precise mechanism underlying the SCF+G-CSF-inhibited post-TBI neurodegeneration remains unclear, a large body of evidence has demonstrated the contribution of SCF and G-CSF in neuroprotection. SCF acts as a neurotrophic factor supporting neuron survival during the development of the peripheral nervous system [29, 45]. SCF [46] or G-CSF [24] protects cultured neurons from excitotoxicity [46] and programmed neuron death [24, 46] through PI3K pathway. Administration of SCF [21], G-CSF [21-26] or SCF+G-CSF [21, 28] in the acute phase of experimental stroke results in infarction size reduction. Neuroprotective effects of G-CSF [47] or SCF+G-CSF [27] treatment in the subacute phase of experimental stroke have also been demonstrated. These studies suggest that SCF+G-CSF-inhibited post-TBI neurodegeneration may be mediated through the similar process of neuroprotection.

Increasing evidence has shown that neural network remodeling in the cortex next to the brain injury area plays a key role in functional recovery [35, 36, 48]. The biological base for the neural network remodeling is brain plasticity that drives reorganization of neural networks after brain injury in either a positive way (adaptive) or a negative way (maladaptive) [49]. The findings of the present study reveals that severe TBI causes reductions of MAP2 positive apical dendrites only in the ipsilateral cortex next to the TBI-cavity but not in the contralateral cortex 24 weeks after TBI induction. SCF+G-CSF treatment in the late subacute phase of TBI leads to increases of the apical dendrites in the peri-TBI cavity cortex. Our previous study, however, has shown that SCF+G-CSF treatment in the subacute phase of TBI (2 weeks post-TBI) prevents the TBI-induced dendritic reduction in the contralateral cortex but not in the ipsilateral cortex [37]. These different findings suggest that SCF+G-CSF treatment-enhanced dendritic growth in the contralateral or in the ipsilateral cortex is dependent on the timing of intervention. Earlier intervention leads to promoting dendritic growth only in the contralateral cortex, whereas later intervention results in enhancing dendritic growth only in the ipsilateral cortex. This view is further supported by our recent study revealing that SCF+G-CSF treatment in the chronic phase of TBI (at 3 months post-TBI) enhances dendritic regeneration only in the peri-TBI cavity cortex but not in the contralateral cortex (Qiu et al., unpublished observations). The apical dendrites of pyramidal neurons in layer II, III and V extend to layer I, and these apical dendrites play a vital role in learning and memory [50]. In chronic stroke studies, in addition to SCF+G-CSF-improved somatosensory motor functional recovery [30], the increased MAP2 positive dendrites are also observed in the peri-infarct cortex after SCF+G-CSF treatment [51]. Surprising findings of the present study are that SMI312 positive axons in the cortex next to the TBI cavity are *increased* in TBI-vehicle control mice as compared to the sham controls. The TBI-induced overgrowth of SMI312 positive axons in this region are prevented by SCF+G-CSF treatment. These *novel* findings suggest that the severe TBI-induced maladaptive (negative) changes in neurostructural networks in the frontal cortex adjacent to the TBI-cavity may be reorganized by SCF+G-CSF treatment in a positive/adaptive way. The frontal cortex, which has functional connections to many brain regions including multiple memory systems such as the hippocampus, has been demonstrated to play a vital role in processing learning, memory, and decision-making [52, 53]. TBI survivors with problems in learning and memory, cognitive function, and decision-making show impaired brain networks in the frontal cortex [54, 55]. Therefore, the positively reorganized

neural networks in the ipsilateral frontal cortex by SCF+G-CSF treatment could be beneficial to the improvement of spatial learning and memory after TBI.

The RAD area comprises the apical dendrites of pyramidal neurons, and the LM region comprises the superficial tufts of the apical dendrites in CA1 [56]. The apical dendrites of CA1 pyramidal neurons in the RAD and LM areas play a key role in cognitive function. The thickness of RAD and LM in the CA1 has been found to be related to delayed recall performance in patients with Alzheimer's disease [57]. In our current study, the severe TBI model causes reductions of apical dendrites in the ipsilateral RAD and LM of the CA1, which is associated with impaired spatial learning and memory. Most importantly, we have also observed the TBI-induced long-term overgrowth of axons in the ipsilateral hippocampal CA1. Similar to our observation, increased axon length and enhanced axon sprouting of granule neurons in the hippocampus have been found in epileptic rodents, which may negatively affect functional characteristics of the hippocampus networks [58-60]. Although SCF+G-CSF treatment has no effects on dendritic density in the hippocampal CA1, the TBI-induced overgrowth of axons in the CA1 of the ipsilateral hemisphere is reduced by SCF+G-CSF treatment, and the axonal density in the ipsilateral CA1 of SCF+G-CSF-treated TBI mice does not show differences with the sham-operative controls. The SCF+G-CSF- prevented axonal overgrowth in the ipsilateral CA1 may be involved in the improvement of cognitive function after severe TBI.

Axon pathology induced by TBI has been well recognized in the field of TBI research. Diffuse axonal injury is a direct consequence of mechanical injury and induces neurodegeneration and functional deficits [61, 62]. In our present long-term TBI study, the axonal injury marker, APP, is not detectable in the brain 24 weeks after TBI, suggesting that the fast axonal transport accumulation of APP may occur only in the acute phase, but not in the late subacute phase of TBI. This view is in line with the findings from other studies showing that APP is upregulated at 1d after TBI, and turns to sparsely expressed at 7d after TBI in mice [63-66]. In humans, APP accumulation is seen within hours after TBI [67]. In the present study, we have discovered a long-term axonal overgrowth in both the peri-TBI cavity frontal cortex and ipsilateral hippocampal CA1 24 weeks after TBI. This abnormal overgrowth of axons may contribute to the TBI-induced long-term impairments in spatial learning and memory. SCF+G-CSF treatment completely prevents the TBI-induced axonal overgrowth. Further studies are warranted to clarify the mechanisms underlying the severe TBI-induced axonal overgrowth and how SCF+G-CSF treatment prevents this unique axonal pathology after TBI.

Conclusions

A single severe TBI in unilateral motor cortex does not only induce motor and cognitive deficits, but also causes long-term and widespread neurodegeneration in bilateral frontal cortex, striatum and hippocampus, and leads to long-term reductions in apical dendrites and axonal overgrowth in the cortex adjacent to the lesion cavity and in the ipsilateral hippocampal CA1. SCF+G-CSF treatment in the late subacute phase of TBI ameliorates the severe TBI-induced long-term severe neuronal pathology, neural network malformation, and impairments in spatial learning and memory. These findings advance our

knowledge of axonal overgrowth in post-TBI pathology, and indicate the therapeutic potential of SCF+G-CSF in restricting severe TBI-caused pathological progression.

Abbreviations

TBI	traumatic brain injury
SCF	Stem cell factor
G-CSF	granulocyte-colony stimulating factor
CCI	Controlled cortical impact
PBS	phosphate buffered saline
NGS	normal goat serum
APP	Amyloid precursor protein
BSA	bovine serum albumin
MAP2	microtubule associated protein 2
RAD	stratum radiatum
LM	stratum lacunosum moleculare

Declarations

Ethics approval

The animal experiments followed ethical guidelines of the Animal Research: Reporting In Vivo Experiments (ARRIVE). All procedures of animal experiments were approved by the Institutional Animal Care and Use Committee and performed in accordance with the National Institutes of Health Guide for the Care and Use of Laboratory Animals.

Consent for publication

Not applicable.

Availability of data and materials

All data are included in the this published article and its supplementary information file.

Competing interests

The authors declare that they have no competing interests. The contents do not represent the views of the U.S. Department of Veterans Affairs or the United States Government.

Funding

This study was supported by Merit Review Award (I01RX002125) from the United States Department of Veterans Affairs Rehabilitation Research & Development Service.

Authors' contributions

JH performed immunohistochemistry and Fluoro-Jade C staining, analyzed the data and wrote the manuscript. TR performed TBI, drug injection, and behavioral tests. XQ and FH performed immunohistochemistry. MK performed H&E staining. LC contributed to study design. LZ designed the study and edited the manuscript.

Acknowledgements

Not applicable.

References

1. Maas AI, Stocchetti N, Bullock R: **Moderate and severe traumatic brain injury in adults**. *The Lancet Neurology* 2008, **7**(8):728-741.
2. Missault S, Anckaerts C, Blockx I, Deleye S, Van Dam D, Barriche N, De Pauw G, Aertgeerts S, Valkenburg F, De Deyn PP *et al*: **Neuroimaging of Subacute Brain Inflammation and Microstructural Changes Predicts Long-Term Functional Outcome after Experimental Traumatic Brain Injury**. *Journal of neurotrauma* 2018.
3. Witcher KG, Bray CE, Dziabis JE, McKim DB, Benner BN, Rowe RK, Kokiko-Cochran ON, Popovich PG, Lifshitz J, Eiferman DS *et al*: **Traumatic brain injury-induced neuronal damage in the somatosensory cortex causes formation of rod-shaped microglia that promote astrogliosis and persistent neuroinflammation**. *Glia* 2018.
4. Ge X, Yu J, Huang S, Yin Z, Han Z, Chen F, Wang Z, Zhang J, Lei P: **A novel repetitive mild traumatic brain injury mouse model for chronic traumatic encephalopathy research**. *Journal of neuroscience methods* 2018, **308**:162-172.
5. Edlow BL, Copen WA, Izzy S, Bakhadirov K, van der Kouwe A, Glenn MB, Greenberg SM, Greer DM, Wu O: **Diffusion tensor imaging in acute-to-subacute traumatic brain injury: a longitudinal analysis**. *BMC neurology* 2016, **16**:2.
6. Rich MC, Keene CN, Neher MD, Johnson K, Yu ZX, Ganivet A, Holers VM, Stahel PF: **Site-targeted complement inhibition by a complement receptor 2-conjugated inhibitor (mTT30) ameliorates post-injury neuropathology in mouse brains**. *Neuroscience letters* 2016, **617**:188-194.
7. Yen TL, Chang CC, Chung CL, Ko WC, Yang CH, Hsieh CY: **Neuroprotective Effects of Platonin, a Therapeutic Immunomodulating Medicine, on Traumatic Brain Injury in Mice after Controlled Cortical Impact**. *International journal of molecular sciences* 2018, **19**(4).

8. Villapol S, Balarezo MG, Affram K, Saavedra JM, Symes AJ: **Neurorestoration after traumatic brain injury through angiotensin II receptor blockage**. *Brain : a journal of neurology* 2015, **138**(Pt 11):3299-3315.
9. Carlson SW, Saatman KE: **Central Infusion of Insulin-Like Growth Factor-1 Increases Hippocampal Neurogenesis and Improves Neurobehavioral Function after Traumatic Brain Injury**. *Journal of neurotrauma* 2018, **35**(13):1467-1480.
10. Anthonymuthu TS, Kenny EM, Lamade AM, Kagan VE, Bayir H: **Oxidized phospholipid signaling in traumatic brain injury**. *Free radical biology & medicine* 2018, **124**:493-503.
11. Hall ED, Sullivan PG, Gibson TR, Pavel KM, Thompson BM, Scheff SW: **Spatial and temporal characteristics of neurodegeneration after controlled cortical impact in mice: more than a focal brain injury**. *Journal of neurotrauma* 2005, **22**(2):252-265.
12. Hall ED, Bryant YD, Cho W, Sullivan PG: **Evolution of post-traumatic neurodegeneration after controlled cortical impact traumatic brain injury in mice and rats as assessed by the de Olmos silver and fluorojade staining methods**. *Journal of neurotrauma* 2008, **25**(3):235-247.
13. Cruz-Haces M, Tang J, Acosta G, Fernandez J, Shi R: **Pathological correlations between traumatic brain injury and chronic neurodegenerative diseases**. *Translational neurodegeneration* 2017, **6**:20.
14. Alhourani A, Wozny TA, Krishnaswamy D, Pathak S, Walls SA, Ghuman AS, Krieger DN, Okonkwo DO, Richardson RM, Niranjan A: **Magnetoencephalography-based identification of functional connectivity network disruption following mild traumatic brain injury**. *Journal of neurophysiology* 2016, **116**(4):1840-1847.
15. Sen T, Gupta R, Kaiser H, Sen N: **Activation of PERK Elicits Memory Impairment through Inactivation of CREB and Downregulation of PSD95 After Traumatic Brain Injury**. *The Journal of neuroscience : the official journal of the Society for Neuroscience* 2017, **37**(24):5900-5911.
16. Rubovitch V, Zilberstein Y, Chapman J, Schreiber S, Pick CG: **Restoring GM1 ganglioside expression ameliorates axonal outgrowth inhibition and cognitive impairments induced by blast traumatic brain injury**. *Scientific reports* 2017, **7**:41269.
17. Greenbaum AM, Link DC: **Mechanisms of G-CSF-mediated hematopoietic stem and progenitor mobilization**. *Leukemia* 2011, **25**(2):211-217.
18. Welte K, Platzer E, Lu L, Gabrilove JL, Levi E, Mertelsmann R, Moore MA: **Purification and biochemical characterization of human pluripotent hematopoietic colony-stimulating factor**. *Proceedings of the National Academy of Sciences of the United States of America* 1985, **82**(5):1526-1530.
19. Zsebo KM, Wypych J, McNiece IK, Lu HS, Smith KA, Karkare SB, Sachdev RK, Yuschenkoff VN, Birkett NC, Williams LR *et al*: **Identification, purification, and biological characterization of hematopoietic stem cell factor from buffalo rat liver–conditioned medium**. *Cell* 1990, **63**(1):195-201.
20. McNiece IK, Briddell RA: **Stem cell factor**. *Journal of leukocyte biology* 1995, **58**(1):14-22.
21. Zhao LR, Singhal S, Duan WM, Mehta J, Kessler JA: **Brain repair by hematopoietic growth factors in a rat model of stroke**. *Stroke* 2007, **38**(9):2584-2591.

22. Six I, Gasan G, Mura E, Bordet R: **Beneficial effect of pharmacological mobilization of bone marrow in experimental cerebral ischemia**. *European journal of pharmacology* 2003, **458**(3):327-328.
23. Shyu WC, Lin SZ, Yang HI, Tzeng YS, Pang CY, Yen PS, Li H: **Functional recovery of stroke rats induced by granulocyte colony-stimulating factor-stimulated stem cells**. *Circulation* 2004, **110**(13):1847-1854.
24. Schneider A, Kruger C, Steigleder T, Weber D, Pitzer C, Laage R, Aronowski J, Maurer MH, Gassler N, Mier W *et al*: **The hematopoietic factor G-CSF is a neuronal ligand that counteracts programmed cell death and drives neurogenesis**. *The Journal of clinical investigation* 2005, **115**(8):2083-2098.
25. Solaroglu I, Tsubokawa T, Cahill J, Zhang JH: **Anti-apoptotic effect of granulocyte-colony stimulating factor after focal cerebral ischemia in the rat**. *Neuroscience* 2006, **143**(4):965-974.
26. Sehara Y, Hayashi T, Deguchi K, Zhang H, Tsuchiya A, Yamashita T, Lukic V, Nagai M, Kamiya T, Abe K: **Decreased focal inflammatory response by G-CSF may improve stroke outcome after transient middle cerebral artery occlusion in rats**. *Journal of neuroscience research* 2007, **85**(10):2167-2174.
27. Kawada H, Takizawa S, Takanashi T, Morita Y, Fujita J, Fukuda K, Takagi S, Okano H, Ando K, Hotta T: **Administration of hematopoietic cytokines in the subacute phase after cerebral infarction is effective for functional recovery facilitating proliferation of intrinsic neural stem/progenitor cells and transition of bone marrow-derived neuronal cells**. *Circulation* 2006, **113**(5):701-710.
28. Toth ZE, Leker RR, Shahar T, Pastorino S, Szalayova I, Asemenew B, Key S, Parmelee A, Mayer B, Nemeth K *et al*: **The combination of granulocyte colony-stimulating factor and stem cell factor significantly increases the number of bone marrow-derived endothelial cells in brains of mice following cerebral ischemia**. *Blood* 2008, **111**(12):5544-5552.
29. Hirata T, Morii E, Morimoto M, Kasugai T, Tsujimura T, Hirota S, Kanakura Y, Nomura S, Kitamura Y: **Stem cell factor induces outgrowth of c-kit-positive neurites and supports the survival of c-kit-positive neurons in dorsal root ganglia of mouse embryos**. *Development (Cambridge, England)* 1993, **119**(1):49-56.
30. Zhao LR, Berra HH, Duan WM, Singhal S, Mehta J, Apkarian AV, Kessler JA: **Beneficial effects of hematopoietic growth factor therapy in chronic ischemic stroke in rats**. *Stroke* 2007, **38**(10):2804-2811.
31. Katafuchi T, Li AJ, Hirota S, Kitamura Y, Hori T: **Impairment of spatial learning and hippocampal synaptic potentiation in c-kit mutant rats**. *Learning & memory (Cold Spring Harbor, NY)* 2000, **7**(6):383-392.
32. Diederich K, Sevimli S, Dorr H, Kosters E, Hoppen M, Lewejohann L, Klocke R, Minnerup J, Knecht S, Nikol S *et al*: **The role of granulocyte-colony stimulating factor (G-CSF) in the healthy brain: a characterization of G-CSF-deficient mice**. *The Journal of neuroscience : the official journal of the Society for Neuroscience* 2009, **29**(37):11572-11581.
33. Zhao LR, Navalitloha Y, Singhal S, Mehta J, Piao CS, Guo WP, Kessler JA, Groothuis DR: **Hematopoietic growth factors pass through the blood-brain barrier in intact rats**. *Experimental neurology* 2007, **204**(2):569-573.

34. Su Y, Cui L, Piao C, Li B, Zhao LR: **The effects of hematopoietic growth factors on neurite outgrowth**. *PloS one* 2013, **8**(10):e75562.
35. Cui L, Duchamp NS, Boston DJ, Ren X, Zhang X, Hu H, Zhao LR: **NF-kappaB is involved in brain repair by stem cell factor and granulocyte-colony stimulating factor in chronic stroke**. *Experimental neurology* 2015, **263**:17-27.
36. Cui L, Wang D, McGillis S, Kyle M, Zhao LR: **Repairing the Brain by SCF+G-CSF Treatment at 6 Months Postexperimental Stroke: Mechanistic Determination of the Causal Link Between Neurovascular Regeneration and Motor Functional Recovery**. *ASN neuro* 2016, **8**(4).
37. Toshkezi G, Kyle M, Longo SL, Chin LS, Zhao LR: **Brain repair by hematopoietic growth factors in the subacute phase of traumatic brain injury**. *Journal of neurosurgery* 2018, **129**(5):1286-1294.
38. Piao CS, Gonzalez-Toledo ME, Gu X, Zhao LR: **The combination of stem cell factor and granulocyte-colony stimulating factor for chronic stroke treatment in aged animals**. *Experimental & translational stroke medicine* 2012, **4**(1):25.
39. Tagge CA, Fisher AM, Minaeva OV, Gaudreau-Balderrama A, Moncaster JA, Zhang XL, Wojnarowicz MW, Casey N, Lu H, Kokiko-Cochran ON *et al*: **Concussion, microvascular injury, and early tauopathy in young athletes after impact head injury and an impact concussion mouse model**. *Brain : a journal of neurology* 2018, **141**(2):422-458.
40. Kondo A, Shahpasand K, Mannix R, Qiu J, Moncaster J, Chen CH, Yao Y, Lin YM, Driver JA, Sun Y *et al*: **Antibody against early driver of neurodegeneration cis P-tau blocks brain injury and tauopathy**. *Nature* 2015, **523**(7561):431-436.
41. Toshkezi G, Kyle M, Longo SL, Chin LS, Zhao LR: **Brain repair by hematopoietic growth factors in the subacute phase of traumatic brain injury**. *Journal of neurosurgery* 2018:1-9.
42. Loane DJ, Kumar A, Stoica BA, Cabatbat R, Faden AI: **Progressive neurodegeneration after experimental brain trauma: association with chronic microglial activation**. *Journal of neuropathology and experimental neurology* 2014, **73**(1):14-29.
43. Pischiutta F, Micotti E, Hay JR, Marongiu I, Sammali E, Tolomeo D, Vegliante G, Stocchetti N, Forloni G, De Simoni MG *et al*: **Single severe traumatic brain injury produces progressive pathology with ongoing contralateral white matter damage one year after injury**. *Experimental neurology* 2018, **300**:167-178.
44. Johnson VE, Stewart W, Arena JD, Smith DH: **Traumatic Brain Injury as a Trigger of Neurodegeneration**. *Advances in neurobiology* 2017, **15**:383-400.
45. Carnahan JF, Patel DR, Miller JA: **Stem cell factor is a neurotrophic factor for neural crest-derived chick sensory neurons**. *The Journal of neuroscience : the official journal of the Society for Neuroscience* 1994, **14**(3 Pt 2):1433-1440.
46. Dhandapani KM, Wade FM, Wakade C, Mahesh VB, Brann DW: **Neuroprotection by stem cell factor in rat cortical neurons involves AKT and NFkappaB**. *Journal of neurochemistry* 2005, **95**(1):9-19.
47. Lee ST, Chu K, Jung KH, Ko SY, Kim EH, Sinn DI, Lee YS, Lo EH, Kim M, Roh JK: **Granulocyte colony-stimulating factor enhances angiogenesis after focal cerebral ischemia**. *Brain research* 2005,

1058(1-2):120-128.

48. Caracciolo L, Marosi M, Mazzitelli J, Latifi S, Sano Y, Galvan L, Kawaguchi R, Holley S, Levine MS, Coppola G *et al*: **CREB controls cortical circuit plasticity and functional recovery after stroke**. *Nature communications* 2018, **9**(1):2250.
49. Zhao LR, Willing A: **Enhancing endogenous capacity to repair a stroke-damaged brain: an evolving field for stroke research**. *Progress in neurobiology* 2018.
50. Spratling MW: **Cortical region interactions and the functional role of apical dendrites**. *Behavioral and cognitive neuroscience reviews* 2002, **1**(3):219-228.
51. Cui L, Murikinati SR, Wang D, Zhang X, Duan WM, Zhao LR: **Reestablishing neuronal networks in the aged brain by stem cell factor and granulocyte-colony stimulating factor in a mouse model of chronic stroke**. *PloS one* 2013, **8**(6):e64684.
52. Badre D, Kayser AS, D'Esposito M: **Frontal cortex and the discovery of abstract action rules**. *Neuron* 2010, **66**(2):315-326.
53. Euston DR, Gruber AJ, McNaughton BL: **The role of medial prefrontal cortex in memory and decision making**. *Neuron* 2012, **76**(6):1057-1070.
54. Kinnunen KM, Greenwood R, Powell JH, Leech R, Hawkins PC, Bonnelle V, Patel MC, Counsell SJ, Sharp DJ: **White matter damage and cognitive impairment after traumatic brain injury**. *Brain : a journal of neurology* 2011, **134**(Pt 2):449-463.
55. Newcombe VF, Outtrim JG, Chatfield DA, Manktelow A, Hutchinson PJ, Coles JP, Williams GB, Sahakian BJ, Menon DK: **Parcellating the neuroanatomical basis of impaired decision-making in traumatic brain injury**. *Brain : a journal of neurology* 2011, **134**(Pt 3):759-768.
56. van Strien NM, Cappaert NL, Witter MP: **The anatomy of memory: an interactive overview of the parahippocampal-hippocampal network**. *Nature reviews Neuroscience* 2009, **10**(4):272-282.
57. Kerchner GA, Deutsch GK, Zeineh M, Dougherty RF, Saranathan M, Rutt BK: **Hippocampal CA1 apical neuropil atrophy and memory performance in Alzheimer's disease**. *NeuroImage* 2012, **63**(1):194-202.
58. Buckmaster PS, Dudek FE: **In vivo intracellular analysis of granule cell axon reorganization in epileptic rats**. *Journal of neurophysiology* 1999, **81**(2):712-721.
59. Buckmaster PS, Dudek FE: **Network properties of the dentate gyrus in epileptic rats with hilar neuron loss and granule cell axon reorganization**. *Journal of neurophysiology* 1997, **77**(5):2685-2696.
60. Zhang S, Khanna S, Tang FR: **Patterns of hippocampal neuronal loss and axon reorganization of the dentate gyrus in the mouse pilocarpine model of temporal lobe epilepsy**. *Journal of neuroscience research* 2009, **87**(5):1135-1149.
61. Johnson VE, Stewart W, Smith DH: **Axonal pathology in traumatic brain injury**. *Experimental neurology* 2013, **246**:35-43.
62. Tsitsopoulos PP, Abu Hamdeh S, Marklund N: **Current Opportunities for Clinical Monitoring of Axonal Pathology in Traumatic Brain Injury**. *Frontiers in neurology* 2017, **8**:599.

63. Bennett RE, Brody DL: **Array tomography for the detection of non-dilated, injured axons in traumatic brain injury**. *Journal of neuroscience methods* 2015, **245**:25-36.
64. Haber M, Hutchinson EB, Sadeghi N, Cheng WH, Namjoshi D, Cripton P, Irfanoglu MO, Wellington C, Diaz-Arrastia R, Pierpaoli C: **Defining an Analytic Framework to Evaluate Quantitative MRI Markers of Traumatic Axonal Injury: Preliminary Results in a Mouse Closed Head Injury Model**. *eNeuro* 2017, **4**(5).
65. Bennett RE, Brody DL: **Acute reduction of microglia does not alter axonal injury in a mouse model of repetitive concussive traumatic brain injury**. *Journal of neurotrauma* 2014, **31**(19):1647-1663.
66. Xia Y, Pu H, Leak RK, Shi Y, Mu H, Hu X, Lu Z, Foley LM, Hitchens TK, Dixon CE *et al*: **Tissue plasminogen activator promotes white matter integrity and functional recovery in a murine model of traumatic brain injury**. *Proceedings of the National Academy of Sciences of the United States of America* 2018, **115**(39):E9230-E9238.
67. Gentleman SM, Nash MJ, Sweeting CJ, Graham DI, Roberts GW: **Beta-amyloid precursor protein (beta APP) as a marker for axonal injury after head injury**. *Neuroscience letters* 1993, **160**(2):139-144.

Additional File Legends

Additional file figure 1. Behavioral testing data one week before treatment initiation. (**A and B**) Quantification data show escape latency to find the platform in the Morris water maze test over 3 days of trials at 2 weeks post-TBI (i.e. one week before treatment). Combined data of 3-day testing show that the escape latency to find the platform is significantly increased in all TBI mice (**A**), but it does not show differences between the randomly-divided two TBI groups (**B**). (**C and D**) Quantification of latency to fall in the Rota-Rod test one week before treatment. Combined data of 3-day testing indicate that the latency to fall is significantly decreased in all TBI mice (**C**), but it does not show differences between the randomly-divided two TBI groups (**D**). $^{*}P<0.05$, $^{**}P<0.01$, Student's t-test.(211KB, pdf)

Additional file figure 2. SCF+G-CSF treatment does not affect brain tissue loss volume after TBI. (**A**) Representative images of the brain sections from the TBI-Vehicle control mice and TBI-SCF+G-CSF-treated mice. Brain sections were stained by H&E. Scale bar, 1mm. (**B**) The percentage of brain tissue loss volume. Student's t-test.(386KB, pdf)

Additional file figure 3. SCF+G-CSF treatment does not affect TBI-induced neuron loss in the ipsilateral cortex and hippocampal CA1. (**A**) Representative images of NeuN immunopositive neurons in the contralateral and ipsilateral cortex. DAPI: nuclear counterstain. Scale bar, 30μm. (**B and C**) Quantification data show the percentage of $NeuN^{+}$ neurons in total of $DAPI^{+}$ cells in the contralateral cortex (**B**) and ipsilateral cortex (**C**). (**D**) Representative images of NeuN immunopositive neurons in the contralateral and ipsilateral CA1. DAPI: nuclear counterstain. Scale bar, 30μm. (**E and F**) Quantification data show the percentage of $NeuN^{+}$ neurons in total of $DAPI^{+}$ cells in the contralateral CA1 (**E**) and ipsilateral CA1 (**F**). $^{*}P<0.05$, one-way ANOVA.(1900KB, pdf)

Additional file figure 4. APP does not accumulate at the late stage of TBI. (**A**) Representative images of APP immunofluorescence staining in the corpus callosum at 24 weeks post-TBI. (**B**) Representative images of APP immunofluorescence staining in the cortex at 24 weeks post-TBI. (**C**) Representative images of APP immunofluorescence staining in the CA1 at 24 weeks post-TBI. (**D**) Representative images of APP immunofluorescence staining in the corpus callosum, cortex and CA1 at 7 days post-TBI. Scale bar, 30 μm. (585KB, pdf)

Figures

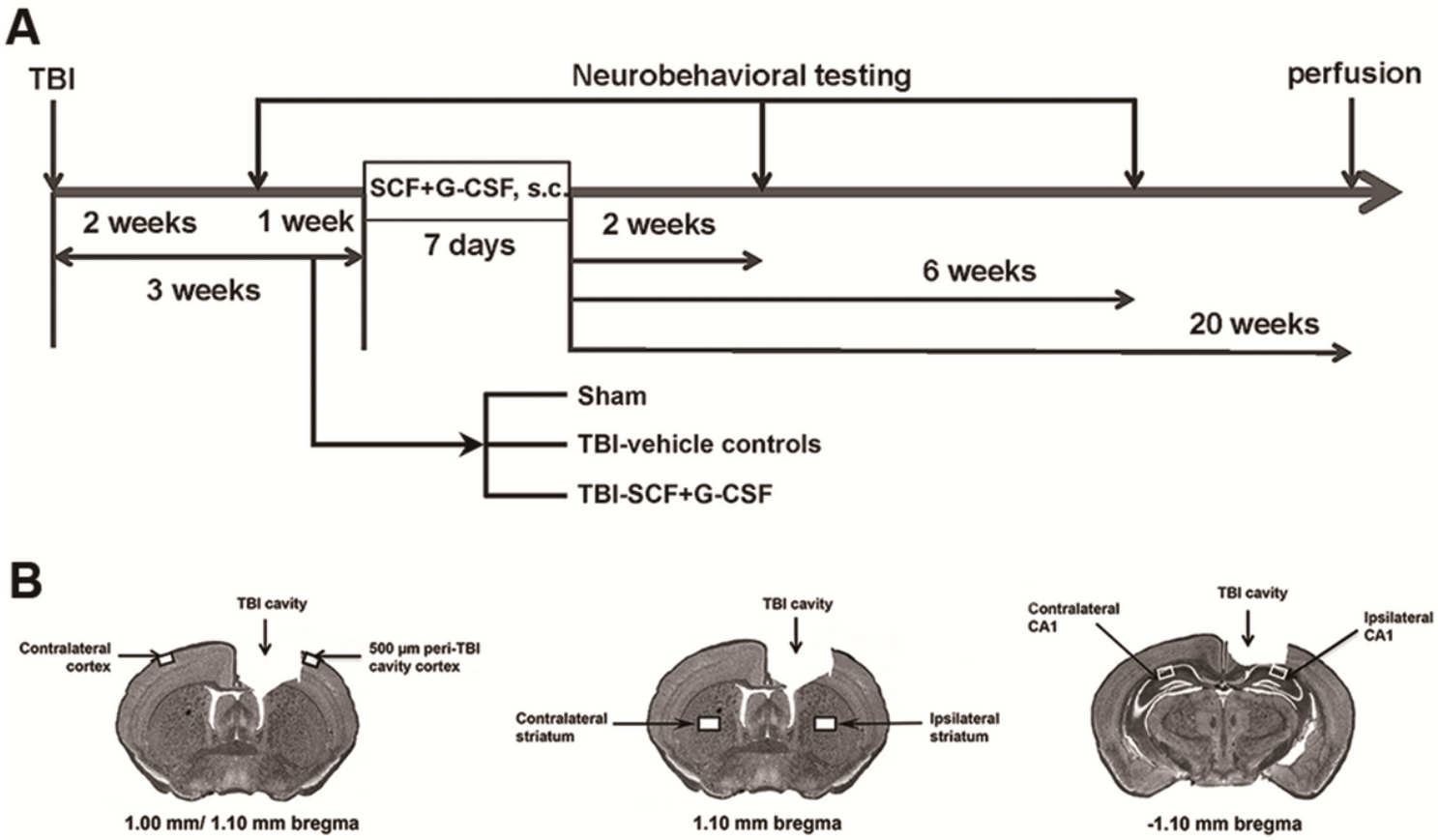

Figure 1

Experimental flowchart and imaging regions. (A) Flowchart of the experiments. Neurobehavioral testing was performed one week before treatment. Based on the findings of neurological deficits, TBI mice were randomly divided into two groups: a vehicle control group and an SCF+G-CSF treatment group. Three weeks after TBI, SCF+G-CSF treatment was subcutaneously (s.c.) administered for 7 consecutive days. Neurological function was evaluated 2 and 6 weeks after the final treatment. Mice were euthanized 20 weeks after the final treatment (i.e. 24 weeks post-TBI). (B) Diagrams show the selected imaging regions in the cortex, striatum and hippocampal CA1.

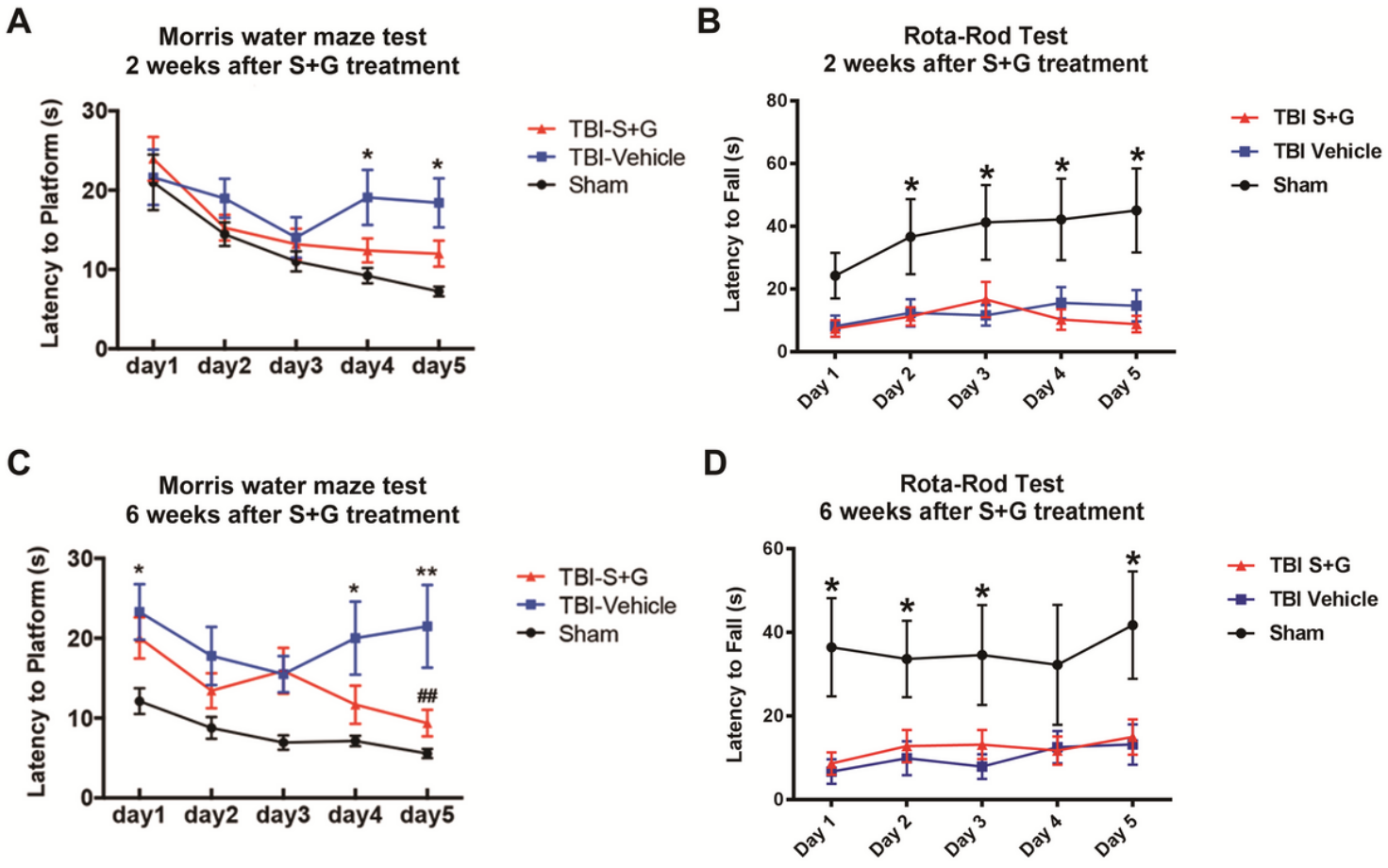

Figure 2

SCF+G-CSF treatment improves TBI-impaired spatial learning and memory but not motor function. (A) The average escape latency to find the platform in a Morris water maze test 2 weeks after SCF+G-CSF treatment. (B) The average time latency to fall from the Rota-Rod 2 weeks after SCF+G-CSF treatment. (C)The average escape latency to find the platform in the Morris water maze test 6 weeks after SCF+G-CSF treatment. (D) The average time latency to fall from the Rota-Rod 6 weeks after SCF+G-CSF treatment. *P<0.05, **P<0.01,TBI-Vehicle mice vs. sham mice. ##P<0.01, TBI-SCF+G-CSF-treated mice vs. TBI-Vehicle control mice. Two-way repeated ANOVA.

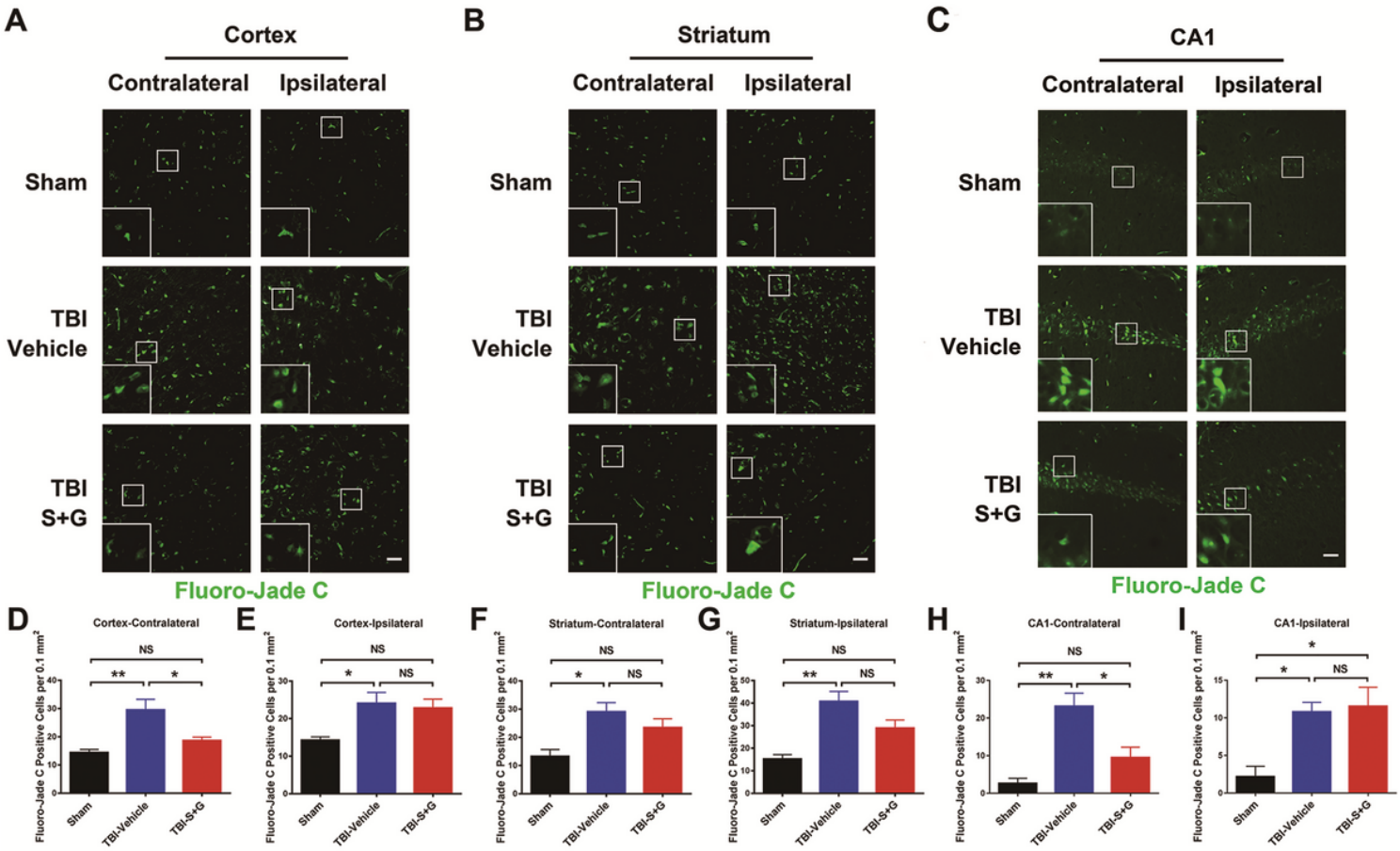

Figure 3

The TBI-increased degenerating neurons are reduced by SCF+G-CSF treatment in the contralateral cortex and hippocampal CA1. (A-C) Representative images of Fluoro-Jade C positive degenerating neurons in the cortex (A), striatum (B), and hippocampal CA1 (C).Scale bar, 30μm. Rectangles: selected areas for showing the magnified images of Fluoro-Jade C positive cells. (D-I) Quantification data of Fluoro-Jade C positive cells per 0.1mm2 in the contralateral cortex (D), ipsilateral cortex next to the TBI cavity (E), contralateral striatum (F), ipsilateral striatum (G), contralateral CA1 (H), and ipsilateral CA1 (I). NS: not significant differences. *P<0.05, **P<0.01, one-way ANOVA.

Figure 4

The TBI-reduced apical dendrites in the ipsilateral cortex adjacent to the TBI cavity is increased by SCF+G-CSF treatment. (A) Representative images of MAP2 immunopositive dendrites in the contralateral cortex. Dashed rectangles: selected areas in cortical layer 1 or layer 2 for the magnified images. Scale bar, 30μm. (B and C) Quantification data of MAP2 immunopositive dendritic optic density in the contralateral cortex. (D and E) Quantification data show the percentage of MAP2 immunopositive area in the contralateral cortex.(F) Representative images of MAP2 immunopositive dendrites in the cortex adjacent to the TBI cavity. Dashed rectangles: selected areas in cortical layer 1 or layer 2 for showing the magnified images. Scale bar, 30μm. (G and H) Quantification data of MAP2 immunopositive dendritic

optic density in the ipsilateral cortex. (I and J) Quantification data illustrate the percentage of MAP2 positive area in the ipsilateral cortex. NS: not significant differences. *P<0.05, **P<0.01, ***P<0.001, one-way ANOVA.

Figure 5

SCF+G-CSF treatment does not affect TBI-reduced apical dendrites in the ipsilateral hippocampal CA1. (A-E) MAP2 immunopositive apical dendrites in the stratum radiatum (RAD) of CA1. (F-J) MAP2 immunopositive apical dendrites in the stratum lacunosum molecular of CA1. (A and F) Representative images of MAP2 immunopositive apical dendrites in the RAD (A) and LM (F) regions of bilateral CA1. Dashed rectangles: selected areas in the RAD or LM region for displaying the magnified images (indicated by arrows). Scale bar, 30μm. (B, D, G, and I) Quantification data of MAP2 positive dendritic optic density in bilateral RAD (B, D) and LM (G, I). (C, E, H and J) Quantification data show the percentage of MAP2 positive area in bilateral RAD (C, E) and LM (H, J). NS: not significant differences. *P<0.05, **P<0.01, one-way ANOVA.

Figure 6

SCF+G-CSF treatment prevents the TBI-induced overgrowth of axons in the ipsilateral cortex. (A) Left panel: Cresyl violet staining illustrates the layers of the cortex. Right panels: Representative images of SMI312 immunopositive axons in bilateral cortex containing layer 1-5 of the three experimental groups. Scale bar, 50μm. (B-D) Quantification data show the percentage of SMI312 immunopositive area at different layers. *P<0.05, **P<0.01,One-way ANOVA.

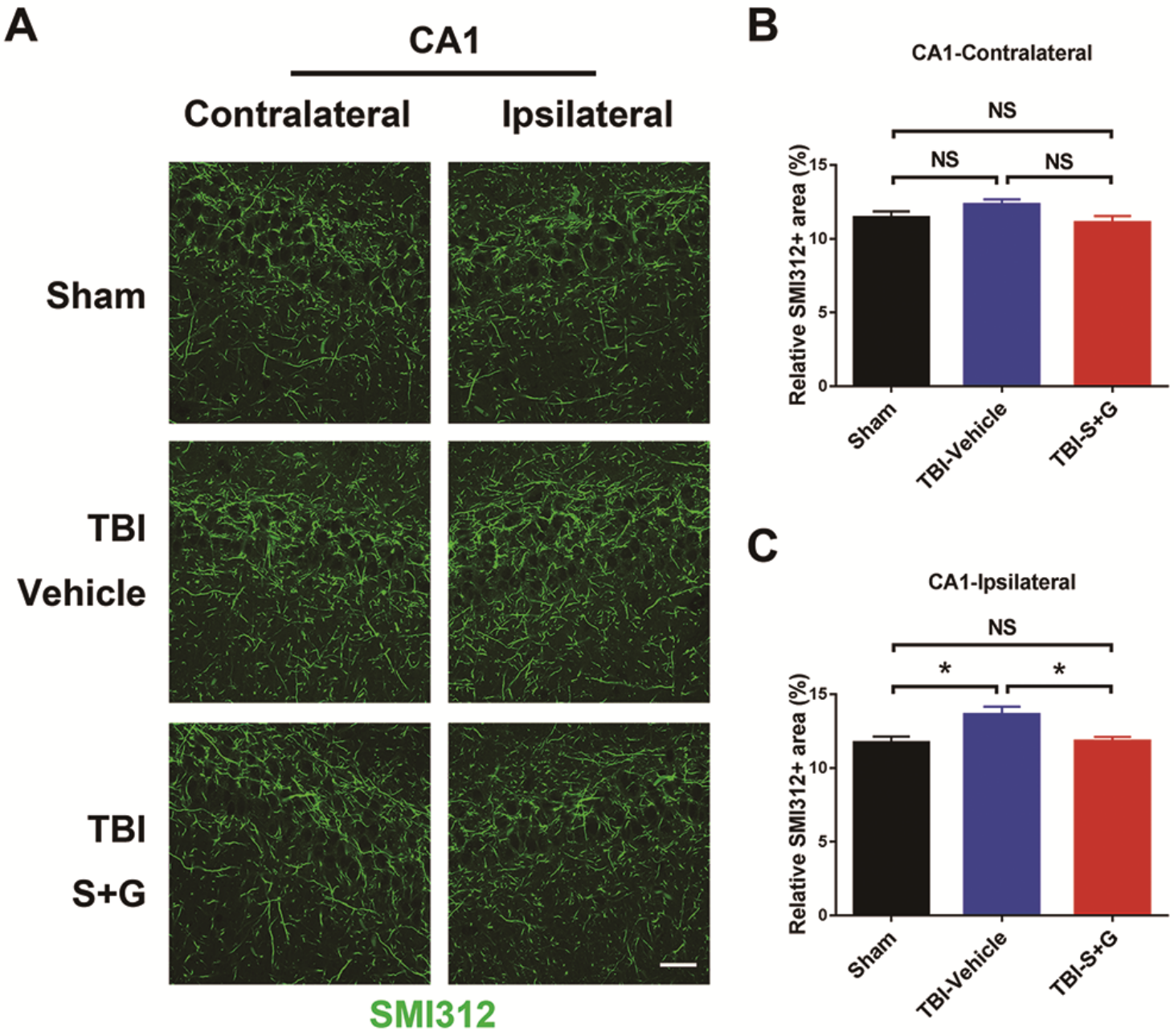

Figure 7

SCF+G-CSF treatment prevents the TBI-induced overgrowth of axons in the ipsilateral hippocampal CA1. (A) Representative images show SMI312 immunopositive axons in bilateral hippocampal CA1. Scale bar, 30μm. (B and C) Quantification data illustrate the percentage of SMI312 immunopositive area in the contralateral CA1 (B) and ipsilateral CA1 (C). NS: not significant differences. *P<0.05, one-way ANOVA.

Supplementary Files

This is a list of supplementary files associated with this preprint. Click to download.

- NC3RsARRIVEGuidelinesChecklist.pdf

- Additionalfile4.pdf
- Additionalfile2.pdf
- Additionalfile1.pdf
- Additionalfile3.pdf